Journal of Hydrology: Regional Studies 48 (2023) 101465

Contents lists available at ScienceDirect

Journal of Hydrology: Regional Studies

journal homepage: www.elsevier.com/locate/ejrh

# A framework to assess future water-resource under climate change in northern Morocco using hydro-climatic modelling and water-withdrawal scenarios

Youness Hrour [a,b], Ophélie Fovet [a], Guillaume Lacombe [b,c], Pauline Rousseau-Gueutin [a,d], Karima Sebari [b], Pascal Pichelin [a], Zahra Thomas [a,*]

[a] Institut Agro, INRAE, SAS, F-35000 Rennes, France
[b] Institut Agronomique et Vétérinaire Hassan II, Département du Génie Rural, Rabat, Morocco
[c] CIRAD, UMR G-EAU, 73 rue JF Breton, F-34398 Montpellier, France
[d] Univ Rennes, EHESP, Rennes, France

ARTICLE INFO

*Keywords:*
Global and regional climate projections
Hydrological GR2M model
Budyko hypothesis
Mediterranean catchment
Uncertainty
EURO-CORDEX

ABSTRACT

*Study region:* The Bas-Loukkos catchment, a Mediterranean catchment in northern Morocco exposed to growing water withdrawal caused mainly by agricultural development.

*Study focus:* For adaptation to climate change, water managers have to consider the high and various uncertainties. To assess impacts of climate change on projected water resources, this study aimed to develop a smart analysis framework to provide scientific information by exploring the complexity of many projections combined with hydrological models. Uncertainties were quantified using 13 pair-wise combinations of 5 regional climate models forced by 4 global climate models under two emissions scenarios (RCP4.5 and RCP8.5), data with and without bias correction (using empirical quantile mapping), and two sets of GR2M hydrological model parameters corresponding to different precipitation conditions. The Budyko hypothesis was used to analyse combined effects of climate change on water resources according to water-withdrawal scenarios. Climate and hydrological projections have been analyzed over three periods: short-term [2020–2040], medium-term [2041–2060] and long-term [2081–2100].

*New hydrological insights for the region:* Results from all simulations indicate that, in the long term (2081–2100), precipitation and discharge will decrease by ca. 21–38% and ca. 50–71%, respectively, compared to the reference period (1981–2005). Consequently, this decline in water resources will require water management strategies to adapt to the future climatic conditions and water demand.

## 1. Introduction

Water resources are facing increasing pressure throughout the world. Agriculture consumes an average of 70% of all freshwater withdrawals (Rosegrant et al., 2009) and up to 95% in some arid and semi-arid countries (Misra, 2013). Water resource availability is strongly limited by the high natural spatio-temporal variability in precipitation and evapotranspiration. Mediterranean regions are highly vulnerable to climate change; almost all models predict that they will experience increased temperatures and decreased

* Corresponding author.
*E-mail address:* zahra.thomas@institut-agro.fr (Z. Thomas).

https://doi.org/10.1016/j.ejrh.2023.101465
Received 18 March 2023; Received in revised form 28 June 2023; Accepted 3 July 2023
Available online 8 July 2023
2214-5818/© 2023 Published by Elsevier B.V. This is an open access article under the CC BY-NC-ND license (http://creativecommons.org/licenses/by-nc-nd/4.0/).

precipitation by the end of the 21st century (García-Ruiz et al., 2011). It is now broadly recognized that the water resources of the Mediterranean region have already been strongly altered by climate change (Balhane et al., 2022; De Girolamo et al., 2022; Senent-Aparicio et al., 2023). Some negative trends have been observed in discharge (El Moçayd et al., 2020; Hrour et al., 2022), while other studies have shown that droughts, more intense and frequent since 1980, have decreased water supplies, agricultural productivity, and electricity production (Verner et al., 2018). According to climate projections, this observed decrease in precipitation and increase in temperature will extend over the 21st century in the Mediterranean region (Tramblay et al., 2020), specifically in Morocco (Balhane et al., 2022; El Khalki et al., 2021a; El Moçayd et al., 2020; Tramblay et al., 2013), with negative effects on water-resource availability (Ayt Ougougdal et al., 2020; Lespinas et al., 2014). Of note, most prospective studies on Mediterranean water resources under climate change were conducted at the regional scale, while water managers have to develop adaptation strategies at the catchment scale.

In Morocco, promotion of irrigated agriculture and improvement of irrigation techniques have led to the expansion of irrigated areas, and the repeated short-term concerns about overexploitation of groundwater are clear (Kuper et al., 2017). The combination of demographic growth, accelerated urbanization, and improved living standards leads to a continuous increase in domestic and industrial water demand (Boretti and Rosa, 2019). Climate models are frequently coupled with hydrological models, including physically based land surface models (Fisher and Koven, 2020), conceptual hydrological models (Pulido-Velazquez et al., 2021), machine learning algorithms (Jimeno-Sáez et al., 2017), in order to propagate hydrological impacts to predict future water resources and develop adaptation strategies, despite multiple sources of uncertainty (Adloff et al., 2015; Lee et al., 2021; Lemaitre-Basset et al., 2021; Senatore et al., 2022). These uncertainties arise from a wide range of sources and propagate throughout impact assessment. They stem first from greenhouse gas (GHG) emission scenarios (i.e. "Representative Concentration Pathways" (RCPs)), then global climate models (GCMs) and their downscaled versions (i.e. regional climate models (RCMs)), followed by bias-correction methods, and finally the hydrological models used to study impacts of climate change on catchment water resources (Adloff et al., 2015; Lee et al., 2021). The main sources of uncertainty are related to climate scenarios (Lee et al., 2021) and the GCMs, which are the main issues hindering the use of climate projections and downscaling procedures (Her et al., 2019; Lee et al., 2021). Therefore, it is recommended to use as many combinations of GCMs, RCMs, and RCP scenarios as possible to better represent multiple sources of uncertainty. Additional sources of uncertainty are the necessarily simplified structure of hydrological models and inaccuracy of the input data used to calibrate them (Lemaitre-Basset et al., 2021; Maraun et al., 2017; Tramblay and Somot, 2018). Uncertainties related to hydrological models are often addressed by using several models that have different structures (Chauveau et al., 2013; Zhou et al., 2021). However, it is now well established that, under non-stationary conditions, additional uncertainties arise from parameter instability caused by changes in climatic conditions of calibrating periods (Coron et al., 2012), unrepresented physical characteristics of catchments, and prevailing processes (Brigode et al., 2013; Lee et al., 2021). Those uncertainties must be taken into account when assessing the impacts of climate change on water resources, in order to develop more appropriate management strategies. However, considering multiple climate and hydrological models, bias-correction methods, and climate scenarios creates a huge number of flow projections. Analysing these abundant projection results thus remains a challenge, and even more so when using such prospective results in management (Carroget et al., 2017). Consequently, the development of a smart analysis framework is needed to provide scientific information by exploring the complexity of many projections. This study aims to propose such a framework for assessing the impacts of climate change on water resources projections in the Bas-Loukkos catchment, a Mediterranean catchment in northern Morocco.

The aim of this study was to develop and evaluate a framework to assess climate change impact on water-resource availability. The first objective was to quantify future changes in precipitation and evapotranspiration and their uncertainties. The second objective was

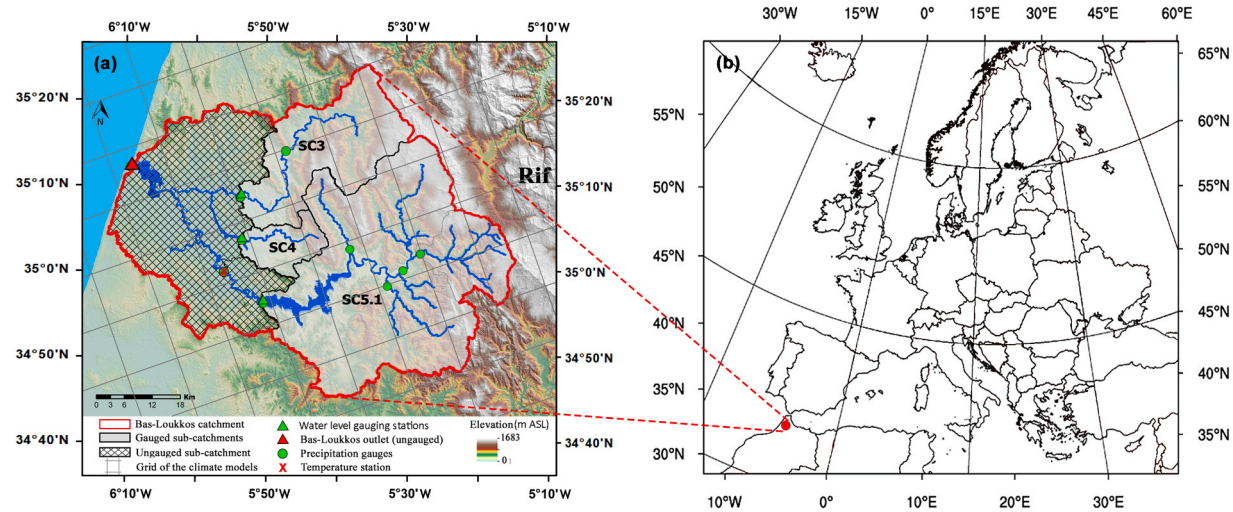


**Fig. 1.** (a) The Bas-Loukkos catchment studied (outlined in red) and the digital elevation model of topography. The catchment is located west of the Rif Mountains. RCM model grids are indicated with the grey cells. (b) The common EURO-CORDEX analysis domain (Jacob et al., 2014) indicating the location of Bas-Loukkos catchment (red point).

to simulate discharge at the catchment scale using climate data from 13 models' outputs and two RCP scenarios according to two parametrizations of the hydrological lumped model. The third objective was to analyse the set of simulated discharge as a function of different agricultural and demographic growth scenarios using the Budyko hypothesis (Budyko, 1974). We thus developed a framework combining data from 13 climate models and two scenarios as input for a lumped hydrological model with two sets of parameters according to two water-withdrawal scenarios.

## 2. Material and methods

### 2.1. Study area

The Bas-Loukkos catchment (3750 km$^2$) is located in north-western Morocco. The eastern part of the catchment is mountainous, with a maximum elevation of 1683 m a.s.l., while the western part is the flat plain of the Bas-Loukkos valley. Loukkos is the main perennial river, running 180 km from the Rif Mountains to the Atlantic Ocean (Fig. 1). Luvisols (39% of the total area) and Vertisols (49% of the total area) dominate the Bas-Loukkos. The climate is sub-humid Mediterranean, with a hot and dry season from May to September and a cool and wet season from October to April, with more than 70% of precipitation occurring during this season. Mean annual precipitation ranges from 616 mm.yr$^{-1}$ in the plain (west) to 1014 mm.yr$^{-1}$ in the Rif Mountains (east). Agriculture is the main economic activity, covering 57% of the area. The agricultural council ORMVAL (*Office Régional de Mise en Valeur Agricole du Loukkos*) is in charge of the development of agriculture in the region. The water agency ABHL (*Agence du Bassin Hydraulique du Loukkos*) is in charge of water distribution and management (dams and irrigated areas). See Hrour et al. (2022) for more detailed description of morphological and climatic characteristics of the catchment.

### 2.2. Observed hydrometeorological data

Precipitation was collected from 10 precipitation stations, while discharge was calculated from three gauging stations which define three sub-catchments: SC3, SC4, and SC5.1 (Fig. 1). Monthly time series data were provided by ABHL and ORMVAL. See Hrour et al. (2022) for more information on the dataset. Potential evapotranspiration (PET) was calculated using the Thornthwaite method (Thornthwaite, 1948) based on temperature data measured at one station (Fig. 1) from 1981 to 2008. As the Bas-Loukkos catchment is not gauged at its outlet, its total discharge was estimated by summing discharge measured at the outlet of the three upstream sub-catchments and the discharge produced in the ungauged downstream section surrounded by the plain. This latter discharge was estimated using transposition (i.e. the drainage area ratio method) (Archfield and Vogel, 2010) (Appendix 1 in the Supplementary material). The discharge (mm) was calculated by dividing the discharge measured at each gauging station by the upstream sub-catchment area.

### 2.3. Future climate projections: climate simulations from EURO-CORDEX

GCMs are used to simulate the global climate system in response to increasing GHG concentrations (Allen et al., 2018; IPCC, 2013) at a coarse resolution (100–500 km) (D'Oria et al., 2017). Impact studies and adaptation strategies, usually developed at the local scale, require much higher resolutions and the use of RCMs. In this study, climate models from the EURO-CORDEX domain (Fig. 1) (http://www.euro-cordex.net) were used, with a spatial resolution of 0.11° (ca. 12 km). This resolution is more appropriate for simulating precipitation of the Euro-Mediterranean region (Fantini et al., 2018; Tramblay et al., 2013). Several studies (i.g. Philipp et al., 2016, 2010; Tramblay et al., 2012) recommend using many models to consider uncertainties arising from the GCMs and the RCMs. To do so, four GCMs (CNRM-CM5, ICHEC-EC-EARTH, MOHC-HadGEM2-ES and MPI-ESM-LR) and five RCMs (CCLM4–8–17, HIRHAM5, RACMO22E, RCA4, REMO2015) were selected. Due to the unavailability of all RCP scenarios, only 13 RCM/GCM combinations (CM01-CM13 in the present study) were used (Table 1). Precipitation and temperature were extracted at a daily time step and then aggregated to a monthly time step. PET was calculated using the Thornthwaite method based on simulated temperature from 2006 to 2099.

Two RCP scenarios from EURO-CORDEX were used (Taylor et al., 2012): RCP4.5 and RCP8.5. The RCP4.5 is the scenario of low-level stabilization, in which radiative forcing is limited to ca. 4.5 W.m$^{-2}$ at the end of the 21st century (IPCC, 2013). The RCP8.5 (business as usual) is the scenario with higher GHG emissions that leads to radiative forcing greater than 8.5 Wm$^{-2}$ (IPCC, 2013).

**Table 1**
The 13 combinations of regional climate models and global climate models used.

| Global climate model | Regional climate models | | | | |
|---|---|---|---|---|---|
| | CCLM4-8–17 | HIRHAM5 | RACMO22E | RCA4 | REMO2015 |
| CNRM-CM5 | ***CM01*** | - | ***CM02*** | ***CM03*** | - |
| ICHEC-EC-EARTH | ***CM04*** | ***CM05*** | ***CM06*** | ***CM07*** | - |
| MOHC-HadGEM2-ES | ***CM08*** | ***CM09*** | ***CM10*** | ***CM11*** | ***CM12*** |
| MPI-M-MPI-ESM-LR | ***CM13*** | - | - | - | - |

### 2.4. Bias correction

Climate model outputs are generally biased (Teutschbein and Seibert, 2012, 2010) due to systematic errors associated with the conceptualization of the models, their spatial discretization, and the averaging of their climate parameters across grid cells. Hence, many authors strongly recommend correcting the biases of GCM and RCM outputs before using them in a hydrological model (Maraun et al., 2017; Smitha et al., 2018; Teutschbein and Seibert, 2012; Willkofer et al., 2018). However, bias-correction methods are based on the strong assumption that the bias in climate model outputs does not change over time (Maraun, 2012). It is impossible to verify this for future climates or regions with arid to semi-arid climates, where precipitation is low and concentrated. In addition, in a climate such as Morocco's, weather fluctuations strongly influence the bias of climate models (Driouech et al., 2010; Tramblay et al., 2013). In addition, bias corrections can introduce artificial trends in climate model outputs, especially for extreme events and precipitation (Maraun, 2013; Themeßl et al., 2012). Therefore, some authors used raw climate model outputs directly in hydrological models (Prudhomme et al., 2010). In the present study, both climate model outputs (with and without bias correction) were used.

Among the several bias-correction methods described in the literature, three methods were tested: linear scaling, gamma quantile mapping, and empirical quantile mapping (EQM) (Cannon et al., 2015; Ivanov and Kotlarski, 2017; Li et al., 2010). When we applied the methods to our model outputs, all three yielded identical results for precipitation, but EQM was clearly the best for temperature; thus, only results from EQM were used (Appendix 2).

The distribution of output simulated by climate models is corrected to match the distribution of observed data (Teutschbein and Seibert, 2012). Means, standard deviations, quantiles, frequencies, and intensities are bias-corrected in a non-linear manner, while extremes remain preserved (Themeßl et al., 2012). For precipitation and temperature, bias correction was performed for the three sub-catchments and each climate model at a monthly time step. The common period for observed and simulated data for precipitation and temperature was 1981–2005, which was considered as the reference period.

### 2.5. GR2M Hydrological modelling

The monthly lumped hydrological model GR2M was used to simulate discharge (Mouelhi et al., 2006). GR2M has two free parameters: X1 (mm), which represents the maximum storage capacity of the soil reservoir (S), and X2 (dimensionless), which represents a coefficient of exchange between surface water and groundwater (see Mouelhi et al., 2006 for more details). Monthly input variables included precipitation (P) and PET. The GR2M model was calibrated and validated for the three gauged sub-catchments SC3, SC4 and SC5.1 (Fig. 1) from 1981 to 2008. The selected calibration-validation period (1981–2008) was split into two non-overlapping periods of equal length. The model was calibrated for period P1 (1981–1994) and P2 (1995–2008) separately, which produced two parameter sets (Parm.01 and Parm.02, respectively). The performance of the model calibrated for each period was then assessed by running the model over the other period. For each calibration period, a 12-month warm-up period was used to initialize internal variables. GR2M was run using the *airGR* package (Coron et al., 2017) of R software (R Core Team, 2021). Based on the standardized precipitation index (Hrour et al., 2022), period P1 was considered very dry, while period P2 had average precipitation conditions with more frequent extreme events. To evaluate the performance of GR2M, the first step was to assess the agreement between simulated and observed high flows using the Nash-Sutcliffe efficiency criterion (NSE) (Nash and Sutcliffe, 1970) (Eq. 5, Appendix 3). High flows were calculated from October to April for each year, as low-flow records contain many null values considered erroneous, as the Loukkos River is perennial. The second step assessed the agreement between simulated and observed discharge (for the entire time series). To do so,

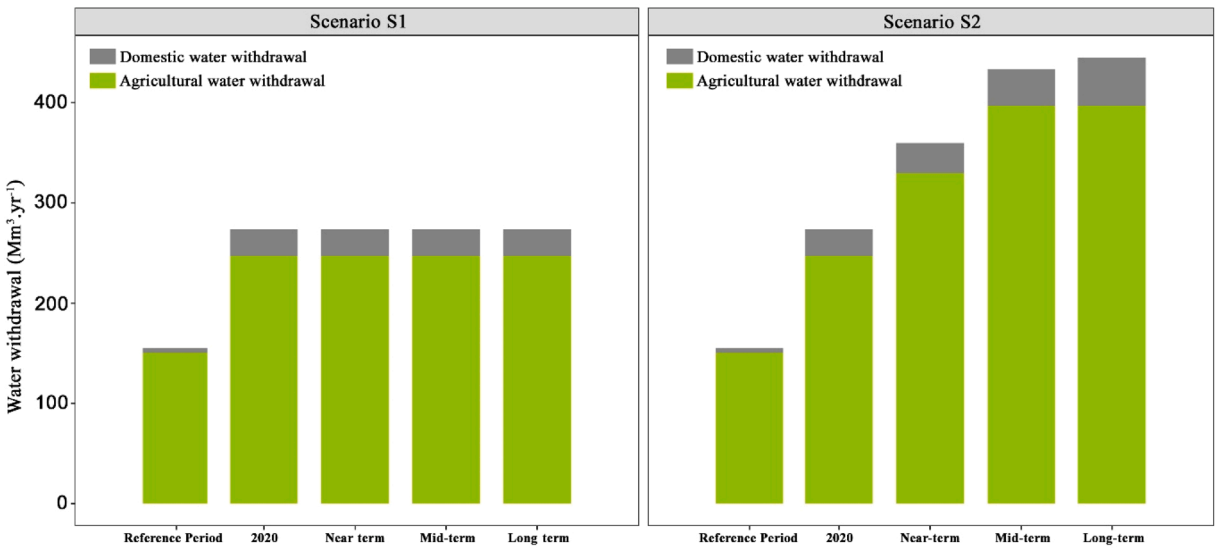


**Fig. 2.** Mean water withdrawals by projection period for the two water-withdrawal scenarios studied.

cumulative error (CE, in %) of simulated and observed discharge was calculated for the entire time series (Eq. 6 in Appendix 3). In addition to the NSE, three other criteria were used to evaluate model performance from 1981 to 2008: the Kling-Gupta Efficiency score (KGE) (Gupta et al., 2009), which combines correlation, variability and bias error (Eq. 7, Appendix 3); root mean square error (RMSE) (Eq. 8, Appendix 3); and percent bias (Pbias) (Eq. 9, Appendix 3).

### 2.6. Statistical analyses

Descriptive statistics (mean, median, standard deviation, inter-quantiles) were used to summarize uncertainties in climate and hydrological projections (Verfaillie et al., 2018), which were analysed over three periods defined in the IPCC's Sixth Assessment Report (Pörtner et al., 2022): near term [2020–2040], mid-term [2041–2060], and long term [2081–2100]. The modified Mann-Kendall trend detection test (M-K test), which considers auto-correlations in time series (Hamed, Ramachandra Rao, 1998; Kendall, 1975; Mann, 1945), and Sen's slope estimator (Sen, 1968) were applied to the annual continuous time series of climate and hydrological model output from 2006 to 2099 to assess potential temporal trends. The trends were considered statistically significant at $p \leq 0.05$. The M-K test and Sen's slope estimator were applied using the function mk.test of the *TREND* package (Libiseller and Grimvall, 2002) of R software.

### 2.7. Future water resource availability

#### 2.7.1. Water demand: two water-withdrawal scenarios

Two water-withdrawal scenarios that summarized changes in water demand were developed based on assumptions about the climate, agricultural development, and population growth (Fig. 2). Due to a lack of data, water withdrawals for industry, currently low

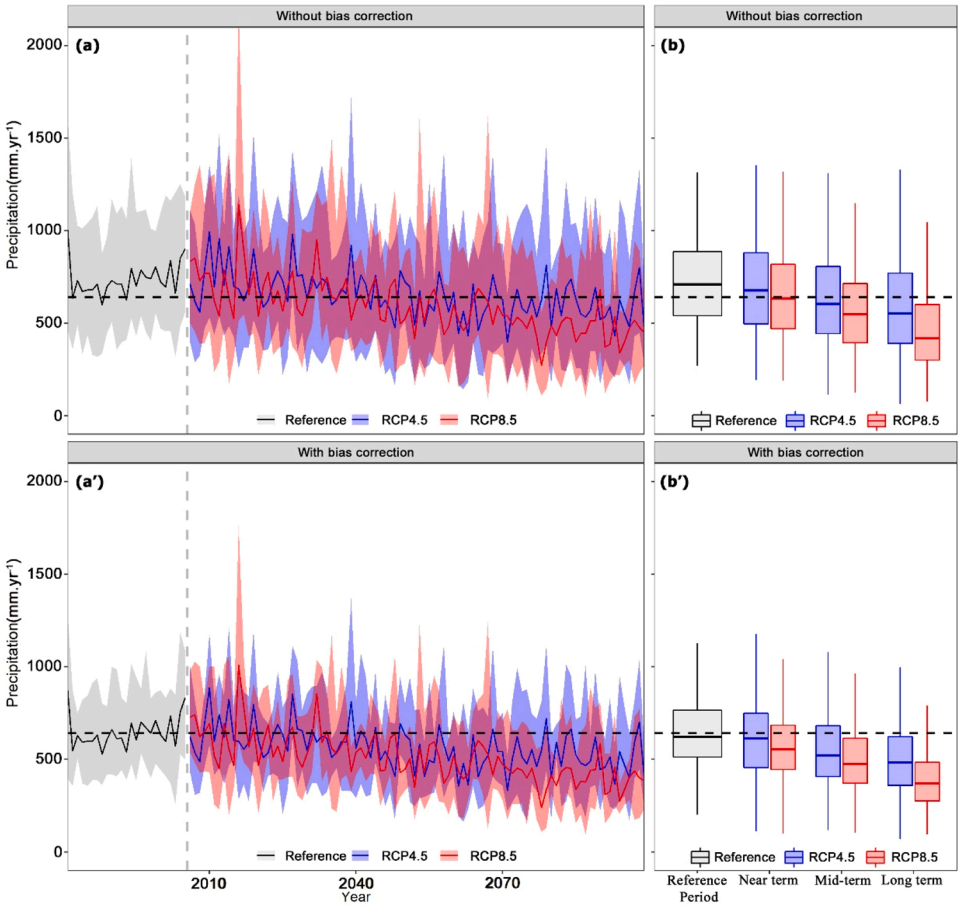


**Fig. 3.** Annual time series of multi-model median (solid lines) and 90th percentile interval (shaded area) of precipitation in the Bas-Loukkos catchment projected under RCP4.5 or RCP8.5 (a) without or (a') with bias correction. Black dashed line: mean observed precipitation from 1981 to 2005. Box-plots of multi-model annual precipitation projected in the near term (2021–2040), mid-term (2041–2060), and long term (2081–2100) under RCP4.5 or RCP 8.5 (b) without or (b') with bias correction compared to the reference period (1981–2005). Whiskers represent the 90th percentile.

in the study catchment, were not considered. In the Bas-Loukkos catchment over the reference period (1981–2005), ABHL and ORMVAL estimated water demands equal to 150 $Mm^3.yr^{-1}$ for agriculture (averaged over 1985–2005) and 5 $Mm^3.yr^{-1}$ for domestic water supply, based on estimates available from 2002 to 2005. In 2020 these demands were estimated at ca. 247 $Mm^3.yr^{-1}$ for agriculture and 27 $Mm^3.yr^{-1}$ for domestic water supply.

Scenario S1 was built from these data and assumed that agriculture and domestic water supply demands would remain constant. This scenario assessed the catchment's ability to support the current water demand in the future, constrained only by climate change. In scenario S2, current demographic trends in the distribution of water use by category in urban and rural areas were extrapolated. Water demand for agriculture was assumed to increase from 247 $Mm^3$ in 2020 to 397 $Mm^3$ in 2030 (ORMVAL and ABHL), and to remain constant from 2030 to 2099. The demand for domestic water supply was assumed to increase linearly from 27 $Mm^3$ in 2020 to 51 $Mm^3$ in 2099.

#### 2.7.2. Budyko hypothesis

The Budyko hypothesis (Budyko, 1974) is a dimensionless graphical representation that describes the annual hydrological cycle based on the relationship between the mean evaporative index (ratio of actual evapotranspiration (AET) to P) and aridity index (ratio of PET to P) in the long term ($\geq$ 10 years). Over the past two decades, the Budyko hypothesis has been widely used in hydrology research (Andréassian et al., 2016; Krajewski et al., 2021; Porporato, 2022) to characterize catchments' water balance and delineate their water and energy limits in order to quantify impacts of climate change and human activities on water availability (Gbohoui et al., 2021). See Appendix 4 for more detailed description.

In the current study, the Budyko hypothesis was used to assess future water availability and characterize the water potential of the Bas-Loukkos catchment under climate change. Mean annual AET was calculated assuming that water storage in the catchment would not change ($\Delta S = 0$) in the long term; thus, AET = P-Q, where Q is the annual discharge at the catchment's outlet. We calculated Q using mean projected discharges in the near, mid- and long term for the RCP4.5 and RCP8.5 scenarios and subtracting the amount of water demanded for agriculture and domestic water uses according to the two water-withdrawal scenarios (S1 and S2).

## 3. Results

### 3.1. Projected inputs

#### 3.1.1. Projected changes in precipitation

The projected annual precipitation time series showed a decreasing trend from 2006 to 2099 under RCP4.5 and RCP8.5 (Fig. 3). However, the trend significance and Sen's slope value depended on the RCPs and climate models (Table 2). The M-K test (Table 2) revealed a significant ($p < 0.05$) decreasing trend in annual precipitation for 8 (RCP4.5) or 13 (RCP8.5) of the 13 climate models (with or without bias correction). The non-significant trend for the remaining five models under RCP4.5 was decreasing for four models (CM01, CM02, CM03, and CM13) and increasing for one model (CM05) (with a Sen's slope of +0.55 $mm.yr^{-1}$ (+0.57 $mm.yr^{-1}$ without bias correction)). Sen's slopes ranged from − 3.13 to − 1.98 $mm.yr^{-1}$ (−4.24 to −1.84 $mm.yr^{-1}$ without bias correction) under RCP4.5 and from − 4.32 to − 1.73 $mm.yr^{-1}$ (−6.14 to −1.64 $mm.yr^{-1}$ without bias correction) under RCP 8.5.

Temporal changes in annual precipitation varied in the near, mid-, and long term (Table 3 and Fig. 3). Compared to the reference period (1981–2005), under RCP4.5, the mean annual precipitation of all models in the near, mid-, and long term decreased by 4%, 14%, and 21%, respectively. Without bias correction, the variation was ca. +11%, -0.5%, and +8%, respectively. With RCP8.5 it caused larger decreases: 9%, 21%, and 38%, respectively. Without bias correction, the variation was ca. +5%, -8%, and -27%, respectively in the near, mid-, and long term. The uncertainty in these changes was ca. 30% with bias correction and ca. 40% without bias correction (Table 3).

**Table 2**
Sen's slopes ($mm.yr^{-1}$) of projected annual precipitation trends in the Bas-Loukkos catchment for each climate model from 2006 to 2099. Bold values are statistically significant (Mann-Kendall trend detection test $p \leq 0.05$).

| Model | Without bias correction | | With bias correction | |
|---|---|---|---|---|
| | RCP4.5 | RCP8.5 | RCP4.5 | RCP8.5 |
| CM01 | -0.53 | **-3.00** | -0.47 | **-3.24** |
| CM02 | -0.42 | **-4.00** | -0.54 | **-3.39** |
| CM03 | -0.97 | **-4.21** | -0.76 | **-3.16** |
| CM04 | **-1.93** | **-1.64** | **-2.46** | **-2.01** |
| CM05 | 0.57 | **-2.01** | 0.55 | **-1.98** |
| CM06 | **-1.84** | **-2.06** | **-1.98** | **-1.97** |
| CM07 | **-2.29** | **-1.82** | **-2.12** | **-1.73** |
| CM08 | **-2.08** | **-3.15** | **-2.28** | **-3.45** |
| CM09 | **-3.17** | **-3.93** | **-3.01** | **-3.86** |
| CM10 | **-3.24** | **-4.26** | **-2.77** | **-3.82** |
| CM11 | **-3.2** | **-4.34** | **-3.03** | **-4.32** |
| CM12 | **-4.24** | **-6.14** | **-3.13** | **-4.32** |
| CM13 | -1.75 | **-3.49** | -1.14 | **-2.33** |

**Table 3**
Absolute (mm) and relative (%) changes and their uncertainty intervals (standard deviation) in mean annual precipitation (P), evapotranspiration (PET), and discharge (Q) in the near term (2021–2040), mid-term (2041–2060), and long term (2081–2100) compared to those of the reference period (1981–2005).

| | Period | Without bias correction | | | | With bias correction | | | |
|---|---|---|---|---|---|---|---|---|---|
| | | RCP4.5 | | RCP8.5 | | RCP4.5 | | RCP8.5 | |
| | | (mm) | (%) | (mm) | (%) | (mm) | (%) | (mm) | (%) |
| P | Near term | + 69 ± 282 | + 11 ± 44 | + 30 ± 256 | + 5 ± 39 | -23 ± 212 | -4 ± 33 | -60 ± 192 | -9 ± 29 |
| | Mid-term | -3 ± 263 | -0.5 ± 41 | -54 ± 257 | -8 ± 40 | -90 ± 203 | -14 ± 31 | -134 ± 193 | -21 ± 30 |
| | Long term | -51 ± 268 | -8 ± 42 | -170 ± 229 | -27 ± 35 | -131 ± 207 | -21 ± 32 | -240 ± 172 | -38 ± 27 |
| PET | Near term | + 59 ± 116 | + 7 ± 13 | + 2 ± 118 | + 0 ± 13 | + 85 ± 61 | + 9 ± 7 | + 32 ± 72 | + 3 ± 8 |
| | Mid-term | + 132 ± 129 | + 15 ± 14 | + 95 ± 128 | + 11 ± 14 | + 141 ± 63 | + 16 ± 7 | + 111 ± 68 | + 12 ± 8 |
| | Long term | + 185 ± 145 | + 21 ± 16 | + 347 ± 194 | + 39 ± 22 | + 184 ± 71 | + 21 ± 8 | + 293 ± 87 | + 33 ± 10 |
| Q | Near term | + 52 ± 193 | + 21 ± 78 | + 28 ± 172 | + 11 ± 70 | -67 ± 115 | -27 ± 47 | -87 ± 96 | -35 ± 39 |
| | Mid-term | + 3 ± 177 | + 1 ± 71 | -32 ± 172 | -13 ± 70 | -102 ± 102 | -41 ± 42 | -125 ± 100 | -51 ± 41 |
| | Long term | -32 ± 170 | -13 ± 69 | -113 ± 134 | -46 ± 55 | -123 ± 98 | -50 ± 40 | -176 ± 70 | -71 ± 30 |

#### *3.1.2. Projected changes in evapotranspiration*

The M-K test revealed significant increases in annual PET from 2006 to 2099 for all climate models and both RCPs (Table S1, Fig. S1). Under RCP4.5, Sen's slope ranged from + 1.21 to + 2.70 mm.yr$^{-1}$ (+1.38 to +4.01 mm.yr$^{-1}$ without bias correction). Under RCP8.5, Sen's slope ranged from + 3.27 to + 5.3 mm.yr$^{-1}$ (+3.65 to +8.34 mm.yr$^{-1}$ without bias correction). Temporal changes in annual PET varied (Table 3): under RCP4.5, the mean annual PET of all models in the near, mid-, and long term increased by 9%, 16%, and 21%, respectively (7%, 15%, and 21%, without bias correction). Under RCP8.5, the mean annual PET increased by 3% 12%, and 33%, respectively (0%, 11%, and 39%, without bias correction). The uncertainty in this change was ca. 10% with bias correction (20% without bias correction) (Table 3).

### *3.2. Projected discharges*

#### *3.2.1. Performance assessment of the GR2M model*

Monthly discharges simulated by GR2M varied (Fig. 4). The resulting model parameters and performance criteria for calibration and validation periods also varied (Table 4). In general, calibration was satisfactory accoding to the KGE, RMSE and Pbias performance criteria. The NSE exceeded 80% for sub-catchments SC3 and SC5.1 for both calibration and validation periods. For sub-catchment SC4, the NSE was ca. 72% for validation period P2 (Table 4). Model parameters varied little between the two periods (X1 by 9% and X2 by 12%), except for sub-catchment SC5.1, for which X1 (i.e. maximum storage capacity of the soil reservoir), increased by 80 mm (i.e. 37%). For calibration periods, the CE ranged from 97.2% to 101.2%, indicating that GR2M simulated discharge correctly. For validation periods, the CE for sub-catchment SC3 equalled 85% and 121% for period P1 and P2, respectively (Table 4), showing that the model calibrated for P1 or P2 underestimated or overestimated, respectively, the discharge over P2 or P1 by ca. 21% or 15%, respectively. For sub-catchment SC4, the CE equalled 70% and 105% for P1 and P2, respectively, showing that calibration for P1 greatly underestimated discharge over P2 (Table 4). For sub-catchment SC5.1, simulated discharge over the validation periods remained close to observations, with a CE of 96% and 95% (Table 4) for P1 and P2, respectively. In general, performance criteria of the two calibration periods differed slightly. The hydrographs showed good agreement between simulated and observed discharges for the three sub-catchments (Fig. 4). In general, GR2M failed to simulate some high-peak events, such as the those observed in all three sub-catchments around December/January in 1984, 1990, 1991, 1996, and 1997 and in sub-catchments SC4 and SC5.1 around March/April in 2003 and 2004.

#### *3.2.2. Projected changes in discharge*

Projected annual discharges (Fig. 5) and trends in projected discharge varied (Table 5). Like for precipitation, trends were significantly decreasing for most climate models and RCPs regardless of the parameter set. Like for precipitation as well, all trends were significant under RCP8.5, while under RCP4.5, four models (CM01, CM02, CM03, and CM13) showed a non-significant decreasing trend for both parameter sets (with and without bias correction), and one model (CM05) showed a non-significant increasing trend. Sen's slopes of all significant trends ranged from − 1.64 to − 0.96 mm.yr$^{-1}$ (−3.06 to −0.98 mm.yr$^{-1}$ without bias correction) under RCP4.5 and from − 2.12 to − 0.80 mm.yr$^{-1}$ (−4.32 to −1.14 mm.yr$^{-1}$ without bias correction) under RCP8.5.

In general, projected discharges decreased throughout the period of projection (Fig. 5). Compared to the reference period, the mean annual discharge from the 13 climate models under RCP4.5 in the near, mid-, and long term, decreased by 27%, 41%, and 50% respectively. Under RCP8.5, this decrease was larger: 35%, 51%, and 71%, respectively in the near, mid-, and long term. Without bias correction, the variation was ca. +21%, +1%, and -13% under RCP4.5 and ca. +11%, -13%, and -46% under RCP8.5, respectively in the near, mid-, and long term. The uncertainty in this change was similar for the two RCPs: ca. 40% with bias correction (ca. 70% without bias correction) (Table 3). Thus, discharges simulated from data with or without bias correction, while lower or higher than those observed during the reference period, respectively, were projected to decrease greatly in the mid- and long term.

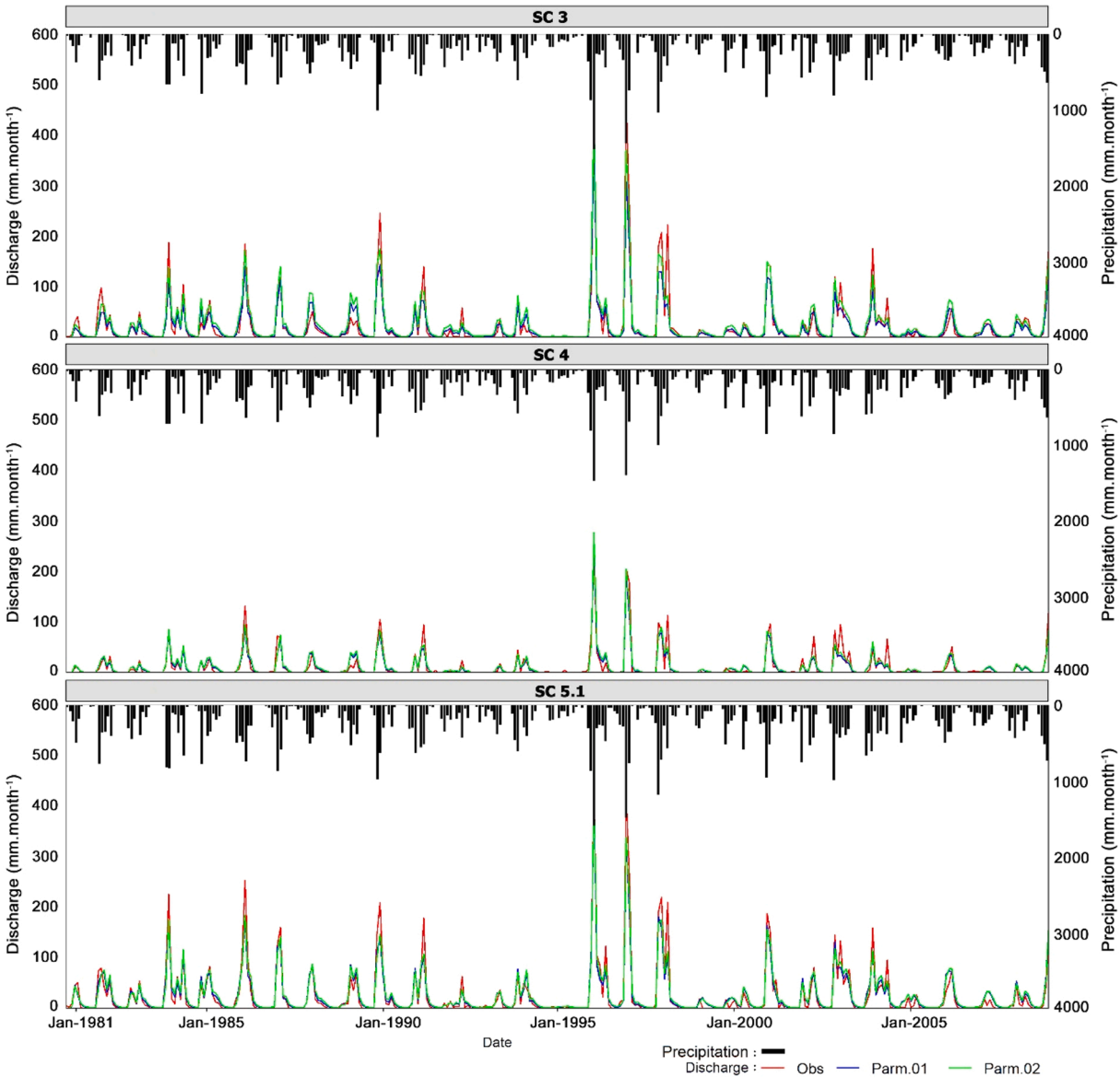


**Fig. 4.** Monthly precipitation, observed discharge, and discharge simulated using parameter sets Parm.01 and Parm.02 (mm month$^{-1}$) for the three sub-catchments SC3, SC4, and SC5.1 over the simulation period (1981–2008).

**Table 4**
Parameters X1 (mm) and X2 (dimensionless) and performance criteria of the GR2M model calibrated for period P1 (1981-1994) or P2 (1995–2008) after calibration (i.e. run for the same period; Cal.) or validation (i.e. run for the other period; Val.), for each sub-catchment simulated.

| Sub-catchment | Calibration period | X1 | X2 | NSE | | RMSE | | KGE | | CE (%) | | Pbias (%) | |
|---|---|---|---|---|---|---|---|---|---|---|---|---|---|
| | | | | Cal. | Val. | Cal. | Val. | Cal. | Val. | Cal. | Val. | Cal. | Val. |
| SC3 | P1 | 224.43 | 0.87 | 0.80 | 0.85 | 16.13 | 25.41 | 0.72 | 0.69 | 97.29 | 85.36 | -2.71 | -14.64 |
| | P2 | 214.4 | 1.00 | 0.91 | 0.81 | 24.76 | 20.36 | 0.88 | 0.74 | 101.20 | 121.24 | 1.20 | 21.24 |
| SC4 | P1 | 250.13 | 0.65 | 0.84 | 0.72 | 7.99 | 24.91 | 0.77 | 0.52 | 100.40 | 70.35 | 0.40 | -29.65 |
| | P2 | 280.41 | 0.71 | 0.9 | 0.85 | 15.08 | 10.00 | 0.91 | 0.8 | 98.53 | 104.90 | -1.47 | 4.90 |
| SC5.1 | P1 | 218.29 | 0.88 | 0.89 | 0.91 | 14.11 | 20.80 | 0.78 | 0.79 | 98.88 | 96.41 | -1.12 | -3.59 |
| | P2 | 291.98 | 0.96 | 0.94 | 0.88 | 21.1 | 18.62 | 0.85 | 0.77 | 100.44 | 94.73 | 0.44 | -5.27 |

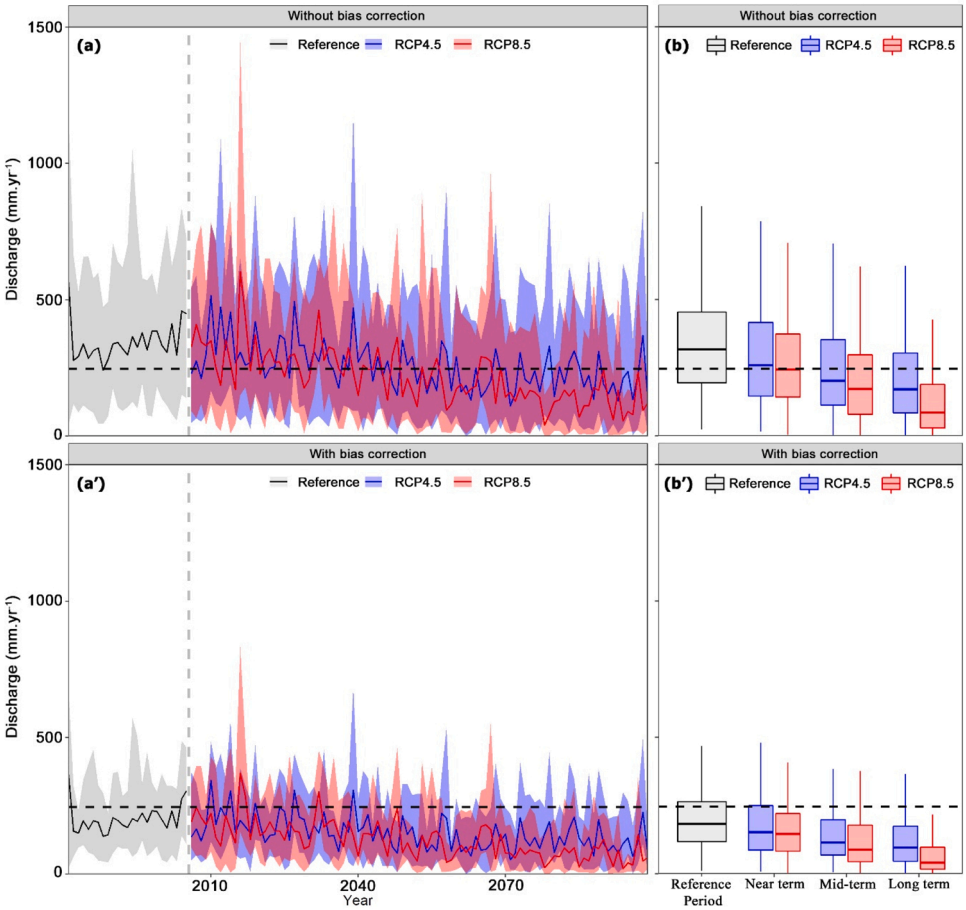


**Fig. 5.** Annual time series of multi-model median (solid curves) and 90th percentile interval (shaded area) of GR2M simulated discharge in the Bas-Loukkos catchment (a) and (a'). Black dashed line: observed annual discharge averaged over 1981–2005. Box-plots of multi-model simulated annual discharge, in the near term (2021–2040), mid-term (2041–2060) and long term (2081–2100), compared to the reference period (1981–2005) (b) and (b'). Whiskers represent the 90th percentile.

**Table 5**
Sen's slopes (mm.yr$^{-1}$) of trends in projected annual discharges in the Bas-Loukkos catchment for each climate model from 2006 to 2099. Bold values are statistically significant (M-K test $p \leq 0.05$). Parm.01 and Parm.02 indicate discharges simulated with the GR2M model calibrated for period P1 or P2, respectively.

| Model | Without bias correction | | | | With bias correction | | | |
|---|---|---|---|---|---|---|---|---|
| | RCP4.5 | | RCP8.5 | | RCP4.5 | | RCP8.5 | |
| | Parm.01 | Parm.02 | Parm.01 | Parm.02 | Parm.01 | Parm.02 | Parm.01 | Parm.02 |
| CM01 | -0.55 | -0.66 | **-2.02** | **-2.32** | -0.52 | -0.60 | **-1.71** | **-1.96** |
| CM02 | -0.74 | -0.89 | **-3.32** | **-3.78** | -0.53 | -0.60 | **-1.88** | **-2.12** |
| CM03 | -1.10 | -1.23 | **-3.34** | **-3.76** | -0.62 | -0.65 | **-1.54** | **-1.76** |
| CM04 | **-0.88** | **-1.00** | **-0.88** | **-0.99** | **-1.10** | **-1.29** | **-1.14** | **-1.29** |
| CM05 | 0.20 | 0.23 | **-1.43** | **-1.63** | 0.09 | 0.12 | **-0.91** | **-1.03** |
| CM06 | **-1.32** | **-1.56** | **-1.42** | **-1.63** | **-1.03** | **-1.19** | **-0.86** | **-0.99** |
| CM07 | **-1.42** | **-1.64** | **-1.31** | **-1.45** | **-0.96** | **-1.10** | **-0.80** | **-0.90** |
| CM08 | **-0.98** | **-1.13** | **-1.14** | **-1.30** | **-1.02** | **-1.15** | **-1.32** | **-1.51** |
| CM09 | **-1.64** | **-1.84** | **-1.97** | **-2.18** | **-1.10** | **-1.27** | **-1.22** | **-1.40** |
| CM10 | **-2.00** | **-2.26** | **-2.63** | **-2.90** | **-1.13** | **-1.30** | **-1.34** | **-1.53** |
| CM11 | **-1.82** | **-2.06** | **-2.44** | **-2.76** | **-1.11** | **-1.31** | **-1.39** | **-1.59** |
| CM12 | **-2.72** | **-3.06** | **-3.84** | **-4.32** | **-1.46** | **-1.64** | **-1.87** | **-2.07** |
| CM13 | -1.04 | -1.17 | **-2.08** | **-2.36** | -0.35 | -0.42 | **-0.86** | **-0.96** |

### 3.3. Effects of uncertainty sources

Effects of the sources of uncertainty considered in this study varied (Fig. 6). For precipitation, PET, and discharge without bias correction (Fig. S2).

#### 3.3.1. Bias corrections

The precipitation and temperature with bias correction best matched the observed data over the reference period. The range of Pbias in precipitation, which was (− 24%)–(46.1%) without bias correction ((−17%) - (−1.3%) for temperature), was reduced to (− 7.5%)–(4.6%) ((0.1%)–(0.2%) for temperature) by bias correction. Bias correction also significantly decreased intra- and inter-model variability (Fig. 5 and S2). For example, precipitation had lower variability and narrower box-plots with bias correction than without. In the long term, mean precipitation with bias correction decreased more than that without bias correction, by 13% (80 mm) for RCP4.5 and 11% (70 mm) for RCP8.5. Like for precipitation, bias correction considerably decreased the variability in simulated discharge. For the reference period (1981–2005), the discharge simulated using data with bias correction was lower than the observed discharge. In the long term, discharge simulated using data with bias correction was lower than that simulated using data without bias correction, by ca. 37% (91 mm) for RCP4.5 and 25% (63 mm) for RCP8.5. The results of the MK test show that bias correction did not suppress the trends observed in the raw data (without bias correction), but it did slightly change the magnitude of that trend. In general, after bias correction, the trends represented by the Sen slope become weaker.

#### 3.3.2. Climate models

The near-, mid-, and long-term projections indicated that interannual variability decreased over time for precipitation and discharge but increased for PET, for all climate models (Fig. 6). In contrast, projections of precipitation, PET, and discharge varied significantly among models (Fig. 6). However, all models projected similar trends: a decrease in precipitation and discharge, and an increase in PET. The uncertainty related to the GCMs exceeded that of RCMs, and this contrast tended to increase over time, as shown in the near-, mid-, and long-term projections. Under RCP4.5, changes in long-term mean precipitation with bias correction varied from − 34% to − 25% (−27% to +25% without bias correction) for GCMs and from − 31% to − 9% (−24% to +15% without bias

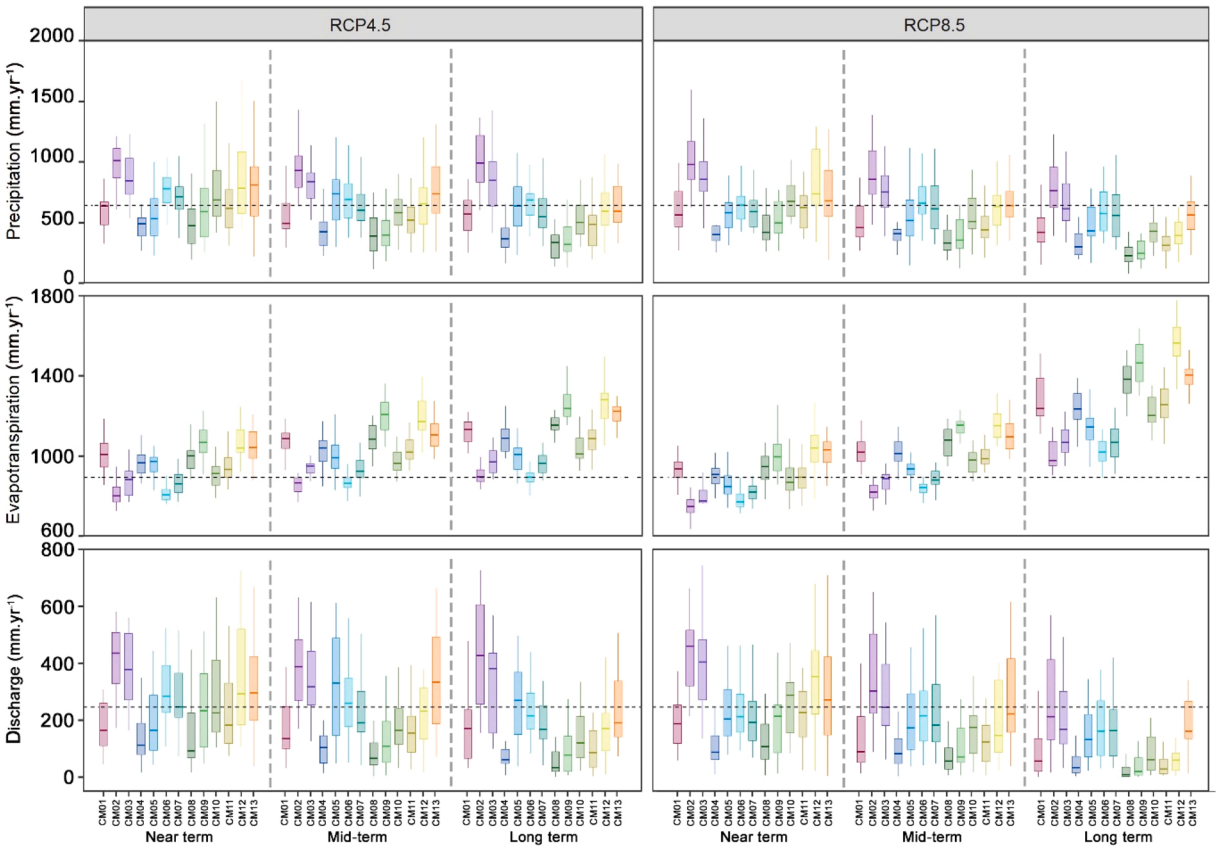


**Fig. 6.** Comparison of sources of uncertainty in annual precipitation, potential evapotranspiration and discharge projected using data without bias correction over the Bas-Loukkos catchment by climate model. Black dashed line: observed mean annual discharge during the reference period [1981–2005]. Whiskers indicate the 90th percentile.

correction) for RCMs. Similar results were found under RCP8.5 for PET and discharge.

#### 3.3.3. GHG scenarios

RCP4.5 and RCP8.5 yielded clearly different precipitation and PET projections, and the difference between the two RCPs increased over time. These differences were also reflected in discharge projections. For precipitation, RCP8.5 yielded a stronger decrease than RCP4.5 for all models (by a mean difference of 30 ± 15 mm in the near and mid-term, and ca. 100 ± 16 mm in the long term). For PET, this difference was larger, especially in the long term (Fig. 6), for which RCP8.5 projected a PET 140 ± 120 mm higher than that of RCP4.5. Similarly, annual discharges simulated using RCP8.5 precipitation and PET data decreased more clearly and strongly than those using RCP4.5 (the mean annual difference of 19 ± 7, 23 ± 8, and 52 ± 5 mm in the near, mid-, and long term, respectively).

#### 3.3.4. GR2M parametrization

Due to hydrological uncertainty during the two calibration periods, parameter sets Parm.01 and Parm.02 differed little (ca. 10 ± 7%), and the difference remained relatively constant over time. The same relative difference between them had previously been observed over the reference period.

### 3.4. The Budyko hypothesis as a tool to assess water availability

For the unchanging water-withdrawal scenario (S1), projections indicated that the water situation in the Bas-Loukkos catchment will become more critical. The evaporative index would increase from 0.63 (reference period) to 0.80 ± 0.16 (near term), then to 0.85 ± 0.18 (mid-term), and to 0.90 ± 0.18 (long term) under RCP4.5, or to 0.81 ± 0.17 (near term), then to 0.89 ± 0.20 (mid-term), and to 1.10 ± 0.22 (long term) under RCP8.5 (Fig. 7). This result suggests that in the mid-term, even maintaining current water demands, the catchment water limit would be reached (evaporative index > 1), with an uncertainty of 15% and 11% under RCP4.5 and RCP8.5, respectively. In the long-term, the catchment water limit would likely be reached for RCP8.5 and with an uncertainty of 1% for RCP4.5.

For trend-based water-withdrawal scenario S2, the Bas-Loukkos catchment would reach its water limit more quickly. The evaporative index would increase from 0.63 (reference period) to 0.84 ± 0.18 (near term), then to 0.93 ± 0.21 (mid-term), and to 1.00 ± 0.22 (long term) under RCP4.5, and to 0.91 ± 0.21 (near term), then to 1.00 ± 0.24 (mid-term), and to 1.18 ± 0.29 (long term) under RCP8.5 (Fig. 7). Thus, the water limits would be reached in the mid-term and exceeded by 18% in the long term under RCP8.5, and would be reached between the mid- and long term under RCP4.5.

For both water-withdrawal scenarios (S1 and S2), the difference between the aridity index under RCP4.5 and RCP8.5 was larger in the long term (1.7 ± 0.85 and 3.6 ± 2.14, respectively), in which the catchment became more arid (Fig. 7). The aridity index increased more than the evaporative index based on the RCPs tested, indicating that the largest change was the increase in water demand and that the catchment would become more arid. Nevertheless, the coefficient of variation was large in the long term, representing 70% of the mean aridity index under RCP8.5 and 55% under RCP4.5.

## 4. Discussion

### 4.1. Simulated discharge from a large set of climate data

The results highlight that, due to climate change, availability of water resources will significantly decrease in the future in the Bas-Loukkos catchment. By the end of the 21st century (2081–2100), discharge will decrease much more (by ca. 50% (RCP4.5) to 71% (RCP8.5)) than precipitation did (by ca. 21% (RCP4.5) to 38% (RCP8.5)) compared to the reference period (1981–2005). This was

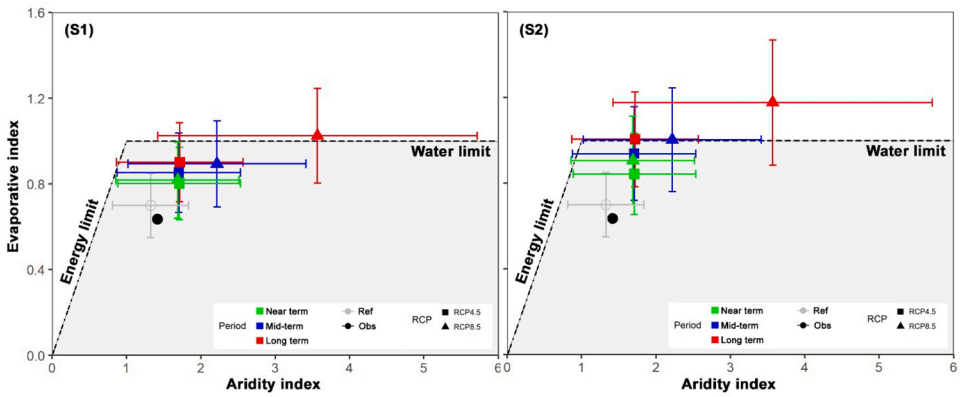


**Fig. 7.** The Budyko hypothesis for the two water-withdrawal scenarios in the Bas-Loukkos catchment under RCP4.5 or RCP8.5. Horizontal error bars represent the standard deviation of the aridity index for all climate models both with and without bias correction. Vertical error bars represent the standard deviation of the evaporative index for all climate models and the two GR2M parameterizations both with and without bias correction.

likely due to the strong increase in temperature, which will cause evapotranspiration to increase. These results agree with other projections for the 21st century in other Moroccan catchments (El Moçayd et al., 2020; Marchane et al., 2017; Tramblay et al., 2013). In particular, El Moçayd et al. (2020) predicted that discharge of the Bas-Loukkos and two neighbouring catchments will decrease by a mean of 44% under RCP4.5 and 90% under RCP8.5 by the end of the 21st century. Their projected decreases may be higher than ours due to the climate or hydrological models chosen and the projected time horizons. Similarly, Marchane et al. (2017) predicted a decrease in surface discharge in the Rheraya catchment (High Atlas, Morocco) of 19–63% depending on the RCP scenario and hydrological model for the horizon 2049–2065. This range of decrease in discharge is similar to those in our mid-term horizon (2041–2060) projection. The discharge decreases projected by these studies, including ours, are relatively high in this region, which is consistent with global climate projections that identify the Mediterranean region as highly vulnerable (Cos et al., 2022). Overall, our results are in line with previous findings in others regions with arid to semi-arid climates. For instance, various studies have reported a decrease in future discharge between 40% and 80% by the end of the 21st century in different regions of Australia (Al-Safi and Sarukkalige, 2018; Usman et al., 2021). Despite the uncertainty, future decreases in discharge are expected to be larger than those observed during the reference period, which experienced severe and prolonged droughts (Hrour et al., 2022). One perspective for this study would be to refine the projections by predicting the seasonality of future discharge (Li et al., 2020).

### 4.2. Future water availability

Future projections provide crucial information for long-term management of water resources and agricultural planning in the region. The Budyko hypothesis analyses combined effects of climate change (discharge trend in response to precipitation and temperature changes) and the two water-withdrawal scenarios, thus capturing all uncertainties. Results suggest that the catchment will likely reach its water limit, with a mean deficit of 1–18% in the long term, depending on the RCP and water-withdrawal scenarios. In the long term, mean total discharge will decrease by ca. 351 $Mm^3$ (RCP4.5) or 584 $Mm^3$ (RCP8.5), while water withdrawal will increase by 119 $Mm^3$ (scenario S1) or 290 $Mm^3$ (scenario S2), compared to those of the reference period, suggesting that the decrease in discharge is the main reason for a water deficit in the catchment in both water-withdrawal scenarios tested. This would result in a shortage of water supply to local users. This is even more crucial as the $86 \times 10^7$ $m^3.yr^{-1}$ expected to be transferred to arid catchments by a planned "water highway" was not considered in the water-withdrawal scenarios. El Moçayd et al. (2020) indicated that transferring water from this catchment to other catchments would be unlikely, as the supply would be too low to satisfy local demand. It is therefore necessary to develop optimal strategies and adapt water-use plans to the future water situation in this catchment. For example, reducing water consumption by limiting the expansion of irrigated areas, adopting other agronomic practices and/or alternative cropping systems (e.g. crops that consume less water, varieties that are more tolerant to water stress and drought). Retaining water and storing it in soils or increasing groundwater recharge may also be considered, but they will likely be insufficient. Technological solutions to increase the effectiveness of water management should be encouraged, but developing adaptation strategies based on understanding the socio-technical functioning of agrosystems and organizations is crucial. In many countries, technology does not reduce social inequality but instead increases pressure on groundwater and may even aggravate problems if applied without considering the socio-economic context (Fischer et al., 2022). In Pakistan, an experiment involving farmers, policy makers, and scientists highlighted the importance of using a multi-stakeholder approach to design interventions and incentives to increase farmers' adaptation to climate change (Javed et al., 2020). This study demonstrated that when farmers are not sensitized to climate change, market-related factors remain the main drivers of agricultural practices. Including climate data in a wide-scale approach to design climate services and decision-making in agriculture is one of the main challenges for disseminating adaptation strategies (Born et al., 2021).

### 4.3. Limitations and perspectives

The perspectives identified to improve the methodological framework developed in this study are related to the bias-correction method, the choice of hydrological model, and the water-withdrawal scenarios. As expected, bias correction successfully reduced biases in projected precipitation and temperature, as well as inter- and intra-model variability. However, discharges projected using data with or without bias correction were lower or higher, respectively, than those observed during the reference period, which highlights the utility of using both data sets (with and without bias correction) to capture uncertainty. This uncertainty may be due to the inability of climate models to represent the seasonality of precipitation in arid and semi-arid regions well, with bias-correction methods correcting only the mean bias well (Meyer et al., 2019; Pierce et al., 2015; Tramblay et al., 2013). Therefore, additional correction methods would be needed to improve projections of climate variability, especially in arid and semi-arid regions.

In this study, only one hydrological model, the conceptual lumped GR2M model, was used, since it requires few input data (Lespinas et al., 2014). However, it does not explicitly represent all hydrological processes that could change in response to climate change (e.g. land use, vegetation uptake, water withdrawal, runoff-infiltration distribution, groundwater-stream water exchange) (Alifujiang et al., 2021; Cristea et al., 2014; Gulahmadov et al., 2021). However, using a unique hydrological model is often the case in studies of the impact of climate change on water resources, particularly in contexts of scarce data (El Khalki et al., 2021b; Ouhamdouch et al., 2019; Tramblay et al., 2013). Therefore, using several hydrological models and different formalisms would provide a good perspective to supplement assessment of hydrological uncertainties, such as by using an approach with more detailed spatial and physical representations (Chauveau et al., 2013; Sharafati and Pezeshki, 2020; Szczypta et al., 2015) or consider the structural uncertainties considering different hydrological conceptual approaches (Pulido-Velazquez et al., 2021). However, these models cannot be applied when data are scarce, as for the Bas-Loukkos catchment. The use of satellite data and remote-sensing products can help

address a lack of data in such cases (Hulsman et al., 2020; Ogilvie et al., 2016).

However, climate change has significant impacts, not only on surface water but on many aspects such as groundwater recharge (Jyrkama and Sykes, 2007), melting ice (Salim et al., 2021), sea-level rise (Mimura, 2013), etc. Furthermore, falling groundwater levels due to overexploitation (Kuper et al., 2017), combined with rising sea levels in coastal areas, are leading to salinization of groundwater. This could further limit available resources (Baena-Ruiz et al., 2020). These effects need to be analyzed using other models, including management models, for enabling the development of really appropriate adaptation strategies (Llopis-Albert and Pulido-Velazquez, 2015; Pulido-Velazquez et al., 2022).

The water-withdrawal scenarios used in this study are simple and do not consider feedback between water-resource availability and water demand. Interactions and feedback between human activities and the water cycle is the subject of current initiatives to develop socio-hydrological models (Blair and Buytaert, 2016; Genova and Wei, 2023) to simulate in a dynamic and realistic way the change in demand according to future water availability.

## 5. Conclusion

Prospective analyses of future water-resource availability at the catchment scale are subject to many and high uncertainties. We were able to quantify these uncertainties using a multi-model approach with 13 climate-model outputs, 2 RCP scenarios, and 2 parameter sets for the GR2M lumped model. Despite these uncertainties, our results project a significant decrease in discharge in the studied catchment by ca. 50–71% by the end of the 21st century, due to a decrease in precipitation and a large increase in evapotranspiration. The Budyko hypothesis indicates that the catchment will reach its water limit; thus, local water demand will be difficult to satisfy in the future, which highlights the need to develop adaptation strategies. This framework was relevant for summarising the projections and their associated uncertainties and then comparing them to potential dynamics of water demand. Thus, such a framework could help guide water-management strategies. Future socio-hydrological studies would be useful to consider dynamic feedback between the water cycle and human uses.

## CRediT authorship contribution statement

**Y.H., Z.T., and O.F.** designed the research; **Y.H., Z.T., O.F., G.L.**, and **P.R.G.** performed the research; **Y.H.** analyzed data; **Y.H., Z.T., O.F., G.L.**, and **P.R.G.** wrote the manuscript; **Y.H and K.S.** provided observed data; **Y.H., Z.T., and P.P.** extracted climate data; and **Y.H.** processed data. The authors declare no conflicts of interest.

## Data Availability

The data from Moroccan agencies can not be shared but all the data from climate models and hydrological simulations are freely available.

## Acknowledgements

Y. Hrour Ph.D. was funded by the PHC Toubkal program (N° TBK/20/95 N°CAMPUS: 43710YB). We thank ABHL and ORMVAL for providing the data and beneficial discussions.

## Appendix A. Supporting information

Supplementary data associated with this article can be found in the online version at doi:10.1016/j.ejrh.2023.101465.

## References

Adloff, F., Somot, S., Sevault, F., Jordà, G., Aznar, R., Déqué, M., Herrmann, M., Marcos, M., Dubois, C., Padorno, E., Alvarez-Fanjul, E., Gomis, D., 2015. Mediterranean Sea response to climate change in an ensemble of twenty first century scenarios. Clim. Dyn. 45, 2775–2802. https://doi.org/10.1007/s00382-015-2507-3.

Alifujiang, Y., Abuduwaili, J., Groll, M., Issanova, G., Maihemuti, B., 2021. Changes in intra-annual runoff and its response to climate variability and anthropogenic activity in the Lake Issyk-Kul Basin, Kyrgyzstan. CATENA 198, 104974. https://doi.org/10.1016/j.catena.2020.104974.

Allen, M.R., O.P. Dube, W. Solecki, F. Aragón-Durand, W. Cramer, S. Humphreys, M. Kainuma, J. Kala, N. Mahowald, Y. Mulugetta, R. Perez, M. Wairiu, and K. Zickfeld, n.d. An IPCC Special Report on the impacts of global warming of 1.5°C above pre-industrial levels and related global greenhouse gas emission pathways, in the context of strengthening the global response to the threat of climate change, sustainable development, and efforts to eradicate poverty. URL ⟨https://www.ipcc.ch/sr15/chapter/chapter-1/⟩ (accessed 11.23.22) (2018).

Al-Safi, H.I.J., Sarukkalige, P.R., 2018. Evaluation of the impacts of future hydrological changes on the sustainable water resources management of the Richmond River catchment. J. Water Clim. Change 9, 137–155.

Andréassian, V., Mander, Ü., Pae, T., 2016. The budyko hypothesis before budyko: the hydrological legacy of evald oldekop. J. Hydrol. 535, 386–391. https://doi.org/10.1016/j.jhydrol.2016.02.002.

Archfield, S.A., Vogel, R.M., 2010. Map correlation method: Selection of a reference streamgage to estimate daily streamflow at ungaged catchments. Water Resour. Res. 46. https://doi.org/10.1029/2009WR008481.

Ayt Ougougdal, H., Yacoubi Khebiza, M., Messouli, M., Lachir, A., 2020. Assessment of future water demand and supply under IPCC climate change and socio-economic scenarios, using a combination of models in ourika watershed, high atlas, morocco. Water 12, 1751. https://doi.org/10.3390/w12061751.

Baena-Ruiz, L., Pulido-Velazquez, D., Collados-Lara, A.-J., Renau-Pruñonosa, A., Morell, I., Senent-Aparicio, J., Llopis-Albert, C., 2020. Summarizing the impacts of future potential global change scenarios on seawater intrusion at the aquifer scale. Environ. Earth Sci. 79, 1–13.

Balhane, S., Driouech, F., Chafki, O., Manzanas, R., Chehbouni, A., Moufouma-Okia, W., 2022. Changes in mean and extreme temperature and precipitation events from different weighted multi-model ensembles over the northern half of Morocco. Clim. Dyn. 58, 389–404. https://doi.org/10.1007/s00382-021-05910-w.

Blair, P., Buytaert, W., 2016. Socio-hydrological modelling: a review asking "why, what and how?". Hydrol. Earth Syst. Sci. 20, 443–478. https://doi.org/10.5194/hess-20-443-2016.

Boretti, A., Rosa, L., 2019. Reassessing the projections of the World Water Development Report. npj Clean. Water 2, 1–6. https://doi.org/10.1038/s41545-019-0039-9.

Born, L., Prager, S., Ramirez-Villegas, J., Imbach, P., 2021. A global meta-analysis of climate services and decision-making in agriculture. Clim. Serv. 22, 100231.

Brigode, P., Oudin, L., Perrin, C., 2013. Hydrological model parameter instability: a source of additional uncertainty in estimating the hydrological impacts of climate change. J. Hydrol. 476, 410–425. https://doi.org/10.1016/j.jhydrol.2012.11.012.

Budyko, M.I., 1974. Climate and life. Academic press.

Cannon, A.J., Sobie, S.R., Murdock, T.Q., 2015. Bias correction of GCM precipitation by quantile mapping: how well do methods preserve changes in quantiles and extremes. J. Clim. 28, 6938–6959. https://doi.org/10.1175/JCLI-D-14-00754.1.

Carroget, A., Perrin, C., Sauquet, É., Vidal, J.-P., Chazot, S., Rouchy, N., Chauveau, M., 2017. Explore 2070: quelle utilisation d'un exercice prospectif sur les impacts des changements climatiques à l'échelle nationale pour définir des stratégies d'adaptation? Sci. Eaux Territ. Numér 22, 4–11. https://doi.org/10.3917/set.022.0004.

Chauveau, M., Chazot, S., Perrin, C., Bourgin, P.-Y., Sauquet, E., Vidal, J.-P., Rouchy, N., Martin, E., David, J., Norotte, T., Maugis, P., Lacaze, X.D., 2013. Quels impacts des changements climatiques sur les eaux de surface en France à l'horizon 2070 ? "What will be the impacts of climate change on surface hydrology in France by 2070 ?". La Houille Blanc 5–15. https://doi.org/10.1051/lhb/2013027.

Coron, L., Andréassian, V., Perrin, C., Lerat, J., Vaze, J., Bourqui, M., Hendrickx, F., 2012. Crash testing hydrological models in contrasted climate conditions: an experiment on 216 Australian catchments. Water Resour. Res. 48 https://doi.org/10.1029/2011WR011721.

Coron, L., Thirel, G., Delaigue, O., Perrin, C., Andréassian, V., 2017. The suite of lumped GR hydrological models in an R package. Environ. Model. Softw. 94, 166–171. https://doi.org/10.1016/j.envsoft.2017.05.002.

Cos, J., Doblas-Reyes, F., Jury, M., Marcos, R., Bretonnière, P.-A., Samsó, M., 2022. The Mediterranean climate change hotspot in the CMIP5 and CMIP6 projections. Earth Syst. Dyn. 13, 321–340. https://doi.org/10.5194/esd-13-321-2022.

Cristea, N.C., Lundquist, J.D., Loheide II, S.P., Lowry, C.S., Moore, C.E., 2014. Modelling how vegetation cover affects climate change impacts on streamflow timing and magnitude in the snowmelt-dominated upper Tuolumne Basin, Sierra Nevada. Hydrol. Process. 28, 3896–3918. https://doi.org/10.1002/hyp.9909.

D'Oria, M., Ferraresi, M., Tanda, M.G., 2017. Historical trends and high-resolution future climate projections in northern Tuscany (Italy). J. Hydrol. 555, 708–723. https://doi.org/10.1016/j.jhydrol.2017.10.054.

De Girolamo, A.M., Barca, E., Leone, M., Lo Porto, A., 2022. Impact of long-term climate change on flow regime in a Mediterranean basin. J. Hydrol.: Reg. Stud. 41, 101061 https://doi.org/10.1016/j.ejrh.2022.101061.

Driouech, F., Déqué, M., Sánchez-Gómez, E., 2010. Weather regimes—moroccan precipitation link in a regional climate change simulation. Glob. Planet. Change 72, 1–10. https://doi.org/10.1016/j.gloplacha.2010.03.004.

El Khalki, E.M., Tramblay, Y., Hanich, L., Marchane, A., Boudhar, A., Hakkani, B., 2021a. Climate change impacts on surface water resources in the Oued El Abid basin, Morocco. Hydrol. Sci. J. 66, 2132–2145. https://doi.org/10.1080/02626667.2021.1982137.

El Khalki, E.M., Tramblay, Y., Hanich, L., Marchane, A., Boudhar, A., Hakkani, B., 2021b. Climate change impacts on surface water resources in the Oued El Abid basin, Morocco. Hydrol. Sci. J. 66, 2132–2145. https://doi.org/10.1080/02626667.2021.1982137.

El Moçayd, N., Kang, S., Eltahir, E.A.B., 2020. Climate change impacts on the Water Highway project in Morocco. Hydrol. Earth Syst. Sci. 24, 1467–1483. https://doi.org/10.5194/hess-24-1467-2020.

Fantini, A., Raffaele, F., Torma, C., Bacer, S., Coppola, E., Giorgi, F., Ahrens, B., Dubois, C., Sanchez, E., Verdecchia, M., 2018. Assessment of multiple daily precipitation statistics in ERA-Interim driven Med-CORDEX and EURO-CORDEX experiments against high resolution observations. Clim. Dyn. 51, 877–900. https://doi.org/10.1007/s00382-016-3453-4.

Fischer, C., Aubron, C., Trouvé, A., Sekhar, M., Ruiz, L., 2022. Groundwater irrigation reduces overall poverty but increases socioeconomic vulnerability in a semiarid region of southern India. Sci. Rep. 12, 8850.

Fisher, R.A., Koven, C.D., 2020. Perspectives on the future of land surface models and the challenges of representing complex terrestrial systems. J. Adv. Model. Earth Syst. 12 e2018MS001453.

García-Ruiz, J.M., López-Moreno, J.I., Vicente-Serrano, S.M., Lasanta–Martínez, T., Beguería, S., 2011. Mediterranean water resources in a global change scenario. Earth-Sci. Rev. 105, 121–139.

Gbohoui, Y.P., Paturel, J.-E., Fowe, Tazen, Mounirou, L.A., Yonaba, R., Karambiri, H., Yacouba, H., 2021. Impacts of climate and environmental changes on water resources: a multi-scale study based on Nakanbé nested watersheds in West African Sahel. J. Hydrol.: Reg. Stud. 35, 100828 https://doi.org/10.1016/j.ejrh.2021.100828.

Genova, P., Wei, Y., 2023. A socio-hydrological model for assessing water resource allocation and water environmental regulations in the Maipo River basin. J. Hydrol. 617, 129159 https://doi.org/10.1016/j.jhydrol.2023.129159.

Gulahmadov, N., Chen, Y., Gulakhmadov, A., Rakhimova, M., Gulakhmadov, M., 2021. Quantifying the relative contribution of climate change and anthropogenic activities on runoff variations in the central part of Tajikistan in Central Asia. Land 10, 525. https://doi.org/10.3390/land10050525.

Gupta, H.V., Kling, H., Yilmaz, K.K., Martinez, G.F., 2009. Decomposition of the mean squared error and NSE performance criteria: Implications for improving hydrological modelling. J. Hydrol. 377, 80–91. https://doi.org/10.1016/j.jhydrol.2009.08.003.

Hamed, K.H., Ramachandra Rao, A., 1998. A modified Mann-Kendall trend test for autocorrelated data. J. Hydrol. 204, 182–196. https://doi.org/10.1016/S0022-1694(97)00125-X.

Her, Y., Yoo, S.-H., Cho, J., Hwang, S., Jeong, J., Seong, C., 2019. Uncertainty in hydrological analysis of climate change: multi-parameter vs. multi-GCM ensemble predictions. Sci. Rep. 9, 4974. https://doi.org/10.1038/s41598-019-41334-7.

Hrour, Y., Thomas, Z., Fovet, O., Sebari, K., Rousseau-Gueutin, P., 2022. Changes in precipitation and discharge in a Mediterranean catchment as a response to climate change and human activities. J. Water Clim. Change 13, 3253–3273. https://doi.org/10.2166/wcc.2022.074.

Hulsman, P., Winsemius, H.C., Michailovsky, C.I., Savenije, H.H.G., Hrachowitz, M., 2020. Using altimetry observations combined with GRACE to select parameter sets of a hydrological model in a data-scarce region. Hydrol. Earth Syst. Sci. 24, 3331–3359. https://doi.org/10.5194/hess-24-3331-2020.

IPCC, W.G.I., 2013. Contribution to the IPCC fifth assessment report. Clim. Change 36.

Ivanov, M.A., Kotlarski, S., 2017. Assessing distribution-based climate model bias correction methods over an alpine domain: added value and limitations. Int. J. Climatol. 37, 2633–2653. https://doi.org/10.1002/joc.4870.

Jacob, D., Petersen, J., Eggert, B., Alias, A., Christensen, O.B., Bouwer, L.M., Braun, A., Colette, A., Déqué, M., Georgievski, G., Georgopoulou, E., Gobiet, A., Menut, L., Nikulin, G., Haensler, A., Hempelmann, N., Jones, C., Keuler, K., Kovats, S., Kröner, N., Kotlarski, S., Kriegsmann, A., Martin, E., van Meijgaard, E., Moseley, C., Pfeifer, S., Preuschmann, S., Radermacher, C., Radtke, K., Rechid, D., Rounsevell, M., Samuelsson, P., Somot, S., Soussana, J.-F., Teichmann, C., Valentini, R., Vautard, R., Weber, B., Yiou, P., 2014. EURO-CORDEX: new high-resolution climate change projections for European impact research. Reg. Environ. Change 14, 563–578. https://doi.org/10.1007/s10113-013-0499-2.

Javed, S.A., Haider, A., Nawaz, M., 2020. How agricultural practices managing market risk get attributed to climate change? Quasi-experiment evidence. J. Rural Stud. 73, 46–55. https://doi.org/10.1016/j.jrurstud.2019.11.020.

Jimeno-Sáez, P., Senent-Aparicio, J., Pérez-Sánchez, J., Pulido-Velazquez, D., Cecilia, J.M., 2017. Estimation of instantaneous peak flow using machine-learning models and empirical formula in peninsular Spain. Water 9, 347.
Jyrkama, M.I., Sykes, J.F., 2007. The impact of climate change on spatially varying groundwater recharge in the grand river watershed (Ontario). J. Hydrol. 338, 237–250. https://doi.org/10.1016/j.jhydrol.2007.02.036.
Kendall, M., 1975. Multivariate analysis. Charles Griffin.
Krajewski, A., Sikorska-Senoner, A.E., Hejduk, L., Banasik, K., 2021. An attempt to decompose the impact of land use and climate change on annual runoff in a small agricultural catchment. Water Resour. Manag. 35, 881–896.
Kuper, M., Amichi, H., Mayaux, P.-L., 2017. Groundwater use in North Africa as a cautionary tale for climate change adaptation. Water Int. 42, 725–740. https://doi.org/10.1080/02508060.2017.1351058.
Lee, S., Qi, J., McCarty, G.W., Yeo, I.-Y., Zhang, X., Moglen, G.E., Du, L., 2021. Uncertainty assessment of multi-parameter, multi-GCM, and multi-RCP simulations for streamflow and non-floodplain wetland (NFW) water storage. J. Hydrol. 600, 126564 https://doi.org/10.1016/j.jhydrol.2021.126564.
Lemaitre-Basset, T., Collet, L., Thirel, G., Parajka, J., Evin, G., Hingray, B., 2021. Climate change impact and uncertainty analysis on hydrological extremes in a French Mediterranean catchment. Hydrol. Sci. J. 66, 888–903. https://doi.org/10.1080/02626667.2021.1895437.
Lespinas, F., Ludwig, W., Heussner, S., 2014. Hydrological and climatic uncertainties associated with modeling the impact of climate change on water resources of small Mediterranean coastal rivers. J. Hydrol. 511, 403–422. https://doi.org/10.1016/j.jhydrol.2014.01.033.
Li, H., Sheffield, J., Wood, E.F., 2010. Bias correction of monthly precipitation and temperature fields from Intergovernmental Panel on Climate Change AR4 models using equidistant quantile matching. J. Geophys. Res.: Atmospheres 115.
Li, Z., Huang, S., Liu, D., Leng, G., Zhou, S., Huang, Q., 2020. Assessing the effects of climate change and human activities on runoff variations from a seasonal perspective. Stoch. Environ. Res Risk Assess. 34, 575–592. https://doi.org/10.1007/s00477-020-01785-1.
Libiseller, C., Grimvall, A., 2002. Performance of partial Mann–Kendall tests for trend detection in the presence of covariates. Environmetrics 13, 71–84. https://doi.org/10.1002/env.507.
Llopis-Albert, C., Pulido-Velazquez, D., 2015. Using MODFLOW code to approach transient hydraulic head with a sharp-interface solution. Hydrol. Process. 29, 2052–2064.
Mann, H.B., 1945. Non-Parametric Tests against Trend. Econmetrica, 13, 245–259. Mantua, NJ, SR Hare, Y. Zhang, JM Wallace, and RC Francis (1997), A Pacific decadal.
Maraun, D., 2012. Nonstationarities of regional climate model biases in European seasonal mean temperature and precipitation sums. Geophys. Res. Lett. 39. https://doi.org/10.1029/2012GL051210.
Maraun, D., 2013. Bias Correction, Quantile Mapping, and Downscaling: Revisiting the Inflation Issue. J. Clim. 26, 2137–2143. https://doi.org/10.1175/JCLI-D-12-00821.1.
Maraun, D., Shepherd, T.G., Widmann, M., Zappa, G., Walton, D., Gutiérrez, J.M., Hagemann, S., Richter, I., Soares, P.M.M., Hall, A., Mearns, L.O., 2017. Towards process-informed bias correction of climate change simulations. Nat. Clim. Change 7, 764–773. https://doi.org/10.1038/nclimate3418.
Marchane, A., Tramblay, Y., Hanich, L., Ruelland, D., Jarlan, L., 2017. Climate change impacts on surface water resources in the Rheraya catchment (High Atlas, Morocco. Hydrol. Sci. J. 62, 979–995. https://doi.org/10.1080/02626667.2017.1283042.
Meyer, J., Kohn, I., Stahl, K., Hakala, K., Seibert, J., Cannon, A.J., 2019. Effects of univariate and multivariate bias correction on hydrological impact projections in alpine catchments. Hydrol. Earth Syst. Sci. 23, 1339–1354. https://doi.org/10.5194/hess-23-1339-2019.
Mimura, N., 2013. Sea-level rise caused by climate change and its implications for society. Proceedings of the Japan Academy, Series B 89, 281–301.
Misra, A.K., 2013. Climate change impact, mitigation and adaptation strategies for agricultural and water resources, in Ganga Plain (India). Mitig. Adapt. Strateg. Glob. Change 18, 673–689.
Mouelhi, S., Michel, C., Perrin, C., Andréassian, V., 2006. Stepwise development of a two-parameter monthly water balance model. J. Hydrol. 318, 200–214. https://doi.org/10.1016/j.jhydrol.2005.06.014.
Nash, J.E., Sutcliffe, J.V., 1970. River flow forecasting through conceptual models part I — A discussion of principles. J. Hydrol. 10, 282–290. https://doi.org/10.1016/0022-1694(70)90255-6.
Ogilvie, A., Belaud, G., Massuel, S., Mulligan, M., Le Goulven, P., Calvez, R., 2016. Assessing Floods and Droughts in Ungauged Small Reservoirs with Long-Term Landsat Imagery. Geosciences 6, 42. https://doi.org/10.3390/geosciences6040042.
Ouhamdouch, S., Bahir, M., Ouazar, D., Carreira, P.M., Zouari, K., 2019. Evaluation of climate change impact on groundwater from semi-arid environment (Essaouira Basin, Morocco) using integrated approaches. Environ. Earth Sci. 78, 1–14.
Philipp, A., Bartholy, J., Beck, C., Erpicum, M., Esteban, P., Fettweis, X., Huth, R., James, P., Jourdain, S., Kreienkamp, F., Krennert, T., Lykoudis, S., Michalides, S.C., Pianko-Kluczynska, K., Post, P., Álvarez, D.R., Schiemann, R., Spekat, A., Tymvios, F.S., 2010. Cost733cat – A database of weather and circulation type classifications. Phys. Chem. Earth, Parts A/B/C., Classif. Atmos. Circ. Patterns – Theory Appl. 35, 360–373. https://doi.org/10.1016/j.pce.2009.12.010.
Philipp, A., Beck, C., Huth, R., Jacobeit, J., 2016. Development and comparison of circulation type classifications using the COST 733 dataset and software. Int. J. Climatol. 36, 2673–2691. https://doi.org/10.1002/joc.3920.
Pierce, D.W., Cayan, D.R., Maurer, E.P., Abatzoglou, J.T., Hegewisch, K.C., 2015. Improved bias correction techniques for hydrological simulations of climate change. J. Hydrometeorol. 16, 2421–2442. https://doi.org/10.1175/JHM-D-14-0236.1.
Porporato, A., 2022. Hydrology without dimensions. Hydrol. Earth Syst. Sci. 26, 355–374.
Pörtner, H.-O., Roberts, D.C., Tignor, M.M.B., Poloczanska, E.S., Mintenbeck, K., Alegría, A., Craig, M., Langsdorf, S., Löschke, S., Möller, V., Okem, A., Rama, B. (Eds.), 2022. Climate Change 2022: Impacts, Adaptation and Vulnerability. Contribution of Working Group II to the Sixth Assessment Report of the Intergovernmental Panel on Climate Change.
Prudhomme, C., Wilby, R.L., Crooks, S., Kay, A.L., Reynard, N.S., 2010. Scenario-neutral approach to climate change impact studies: application to flood risk. J. Hydrol. 390, 198–209. https://doi.org/10.1016/j.jhydrol.2010.06.043.
Pulido-Velazquez, D., Collados-Lara, A.J., Pérez-Sánchez, J., Segura-Méndez, F.J., Senent-Aparicio, J., 2021. Climate change impacts on the streamflow in Spanish basins monitored under near-natural conditions. J. Hydrol.: Reg. Stud. 38, 100937.
Pulido-Velazquez, D., Collados-Lara, A.-J., Fernandez-Chacon, F., 2022. The impact of climate change scenarios on droughts and their propagation in an arid Mediterranean basin. A useful approach for planning adaptation strategies. Sci. Total Environ. 820, 153128.
Rosegrant, M.W., Ringler, C., Zhu, T., 2009. Water for agriculture: maintaining food security under growing scarcity. Annu. Rev. Environ. Resour. 34, 205–222.
Salim, E., Ravanel, L., Deline, P., Gauchon, C., 2021. A review of melting ice adaptation strategies in the glacier tourism context. Scand. J. Hosp. Tour. 21, 229–246.
Sen, P.K., 1968. Estimates of the regression coefficient based on Kendall's tau. J. Am. Stat. Assoc. 63, 1379–1389.
Senatore, A., Fuoco, D., Maiolo, M., Mendicino, G., Smiatek, G., Kunstmann, H., 2022. Evaluating the uncertainty of climate model structure and bias correction on the hydrological impact of projected climate change in a Mediterranean catchment. J. Hydrol.: Reg. Stud. 42, 101120 https://doi.org/10.1016/j.ejrh.2022.101120.
Senent-Aparicio, J., López-Ballesteros, A., Jimeno-Sáez, P., Pérez-Sánchez, J., 2023. Recent precipitation trends in Peninsular Spain and implications for water infrastructure design. J. Hydrol.: Reg. Stud. 45, 101308 https://doi.org/10.1016/j.ejrh.2022.101308.
Sharafati, A., Pezeshki, E., 2020. A strategy to assess the uncertainty of a climate change impact on extreme hydrological events in the semi-arid Dehbar catchment in Iran. Theor. Appl. Clim. 139, 389–402. https://doi.org/10.1007/s00704-019-02979-6.
Smitha, P.S., Narasimhan, B., Sudheer, K.P., Annamalai, H., 2018. An improved bias correction method of daily rainfall data using a sliding window technique for climate change impact assessment. J. Hydrol. 556, 100–118. https://doi.org/10.1016/j.jhydrol.2017.11.010.
Szczypta, C., Gascoin, S., Houet, T., Hagolle, O., Dejoux, J.-F., Vigneau, C., Fanise, P., 2015. Impact of climate and land cover changes on snow cover in a small Pyrenean catchment. J. Hydrol. 521, 84–99. https://doi.org/10.1016/j.jhydrol.2014.11.060.
Taylor, K.E., Stouffer, R.J., Meehl, G.A., 2012. An overview of CMIP5 and the experiment design. Bull. Am. Meteorol. Soc. 93, 485–498. https://doi.org/10.1175/BAMS-D-11-00094.1.

Teutschbein, C., Seibert, J., 2010. Regional Climate Models for Hydrological Impact Studies at the Catchment Scale: A Review of Recent Modeling Strategies. Geogr. Compass 4, 834–860. https://doi.org/10.1111/j.1749-8198.2010.00357.x.

Teutschbein, C., Seibert, J., 2012. Bias correction of regional climate model simulations for hydrological climate-change impact studies: Review and evaluation of different methods. J. Hydrol. 456–457, 12–29. https://doi.org/10.1016/j.jhydrol.2012.05.052.

Themeßl, M.J., Gobiet, A., Heinrich, G., 2012. Empirical-statistical downscaling and error correction of regional climate models and its impact on the climate change signal. Clim. Change 112, 449–468. https://doi.org/10.1007/s10584-011-0224-4.

Thornthwaite, C.W., 1948. An approach toward a rational classification of climate. Geogr. Rev. 38, 55–94.

Tramblay, Y., Somot, S., 2018. Future evolution of extreme precipitation in the Mediterranean. Clim. Change 151, 289–302. https://doi.org/10.1007/s10584-018-2300-5.

Tramblay, Y., Badi, W., Driouech, F., El Adlouni, S., Neppel, L., Servat, E., 2012. Climate change impacts on extreme precipitation in Morocco. Glob. Planet. Change 82–83, 104–114. https://doi.org/10.1016/j.gloplacha.2011.12.002.

Tramblay, Y., Ruelland, D., Somot, S., Bouaicha, R., Servat, E., 2013. High-resolution Med-CORDEX regional climate model simulations for hydrological impact studies: a first evaluation of the ALADIN-Climate model in Morocco. Hydrol. Earth Syst. Sci. 17, 3721–3739. https://doi.org/10.5194/hess-17-3721-2013.

Tramblay, Y., Llasat, M.C., Randin, C., Coppola, E., 2020. Climate change impacts on water resources in the Mediterranean. s10113-020-01665-y Reg. Environ. Change 20 (83). https://doi.org/10.1007/s10113-020-01665-y.

Usman, M., Ndehedehe, C.E., Farah, H., Manzanas, R., 2021. Impacts of climate change on the streamflow of a large river basin in the Australian tropics using optimally selected climate model outputs. J. Clean. Prod. 315, 128091 https://doi.org/10.1016/j.jclepro.2021.128091.

Verfaillie, D., Lafaysse, M., Déqué, M., Eckert, N., Lejeune, Y., Morin, S., 2018. Multi-component ensembles of future meteorological and natural snow conditions for 1500 m altitude in the Chartreuse mountain range, Northern French Alps. Cryosphere 12, 1249–1271.

Verner, D., Treguer, D., Redwood, J., Christensen, J., McDonnell, R., Elbert, C., Konishi, Y., Belghazi, S., 2018. Climate Variability, Drought, and Drought Management in Morocco's Agricultural Sector (Working Paper). World Bank, Washington, DC. https://doi.org/10.1596/30603.

Willkofer, F., Schmid, F.-J., Komischke, H., Korck, J., Braun, M., Ludwig, R., 2018. The impact of bias correcting regional climate model results on hydrological indicators for Bavarian catchments. J. Hydrol.: Reg. Stud. 19, 25–41. https://doi.org/10.1016/j.ejrh.2018.06.010.

Zhou, S., Wang, Y., Li, Z., Chang, J., Guo, A., 2021. Quantifying the uncertainty interaction between the model input and structure on hydrological processes. Water Resour. Manag. 35, 3915–3935. https://doi.org/10.1007/s11269-021-02883-7.